INVESTIGATION OF THE EXPANSION OF NICKEL VERSUS TEMPERATURE BY X-RAY ANALYSIS

by

ELLIOT RODNEY BABCOCK

B. S., Kansas State College
of Agriculture and Applied Science, 1949

A THESIS

submitted in partial fulfillment of the

requirements for the degree

MASTER OF SCIENCE

Department of Physics

KANSAS STATE COLLEGE
OF AGRICULTURE AND APPLIED SCIENCE

1950

TABLE OF CONTENTS

INTRODUCTION

Much research has been conducted on ferromagnetic substances in an effort to determine what happens to them at their Curie temperatures. This is the temperature at which a ferromagnetic material undergoes a transition to the paramagnetic state. An abrupt change in many of the physical properties of the material has been observed at this point. This was exemplified by the research conducted on the photoelectric properties of nickel by Cardwell (3) in 1949. In an effort to find some possible cause for these discontinuities as found by Cardwell, it was decided to investigate the linear thermal expansion of nickel around the Curie temperature. This was to be done by using x-ray diffraction analysis, which would also enable one to investigate any crystallographic changes which might occur, along with the microscopic investigation of the thermal expansion. For this problem a high temperature powder camera had to be constructed.

Since the discovery of x-ray diffraction, many substances have been investigated by x-ray analysis, including nickel. It was found that nickel occurred in two crystallographic forms. It is most generally found to exist as face-centered cubic crystals; however, it has been reported to exist in the form of hexagonal crystals. In 1925, Del Regno (6) reported that the transformation of nickel from the ferromagnetic to the paramagnetic state, along with the accompanying changes

in other physical properties, seemed not to occur at any one definite temperature; but it occupied a range of temperatures extending from 300 degrees to 400 degrees Centigrade. Since then the temperature at which these changes occur has been fairly well determined and is called the Curie temperature. Mazza and Nasini (10) used several methods for the crystallization of nickel in 1929 and found that the nickel always crystallized into face-centered cubes. Sizoo (13), in 1929, investigated the magnetic properties of nickel as a function of crystal size. He obtained similar results for nickel and iron. Hexagonal nickel was prepared by Bredig and von Bergkampf (2) in 1931. It was found to be nonmagnetic, but upon heating it to 300 degrees Centigrade, it was transformed into magnetic nickel with a face-centered cubic lattice. Del Nunzio (5) determined nickel to be face-centered cubic and also found that x-ray analysis did not elucidate changes in the magnetic behavior. Observations of the cubic form of nickel by Koester and Schmidt (9) in 1934 showed a decrease of volume of about 1.0 percent per atom during the transition from the ferromagnetic to the paramagnetic state. In 1934, Jesse (8) took x-ray powder photographs of a heated cubic nickel sample over the temperature range from 450 degrees to 1200 degrees Centigrade. He found no new forms of nickel within this range. The thermal expansion of the face-centered cubic lattice agreed with the microscopic thermal expansion data. Williams (15), in 1934, made general studies of the coefficient of thermal expansion between 200 degrees and

500 degrees Centigrade. A detailed investigation of the thermal expansion was made of the nickel near its Curie temperature. He found the coefficient of expansion to reach a maximum at about 355 degrees Centigrade and then suddenly to decrease for larger temperatures.

Ewert (7), in 1936, showed from results of calorimetric measurements of the specific heat in the temperature range 196 degrees to 948 degrees Centigrade that the field of stable existence for the hexagonal form of nickel was between 345 degrees and 351 degrees Centigrade. However, he concluded that the change of nickel from the ferromagnetic to the feebly paramagnetic state was not accompanied by a change in the crystal structure. Owen and Yates (12) determined the expansion of the nickel lattice by x-ray analysis in 1936. They covered the range of temperatures from 12 degrees to 600 degrees. The coefficient of expansion began to increase abnormally at 320 degrees, reached a maximum at 370 degrees which is near the temperature of magnetic transformation, and then dropped suddenly to a normal value at around 390 degrees. Nix and MacNair (11) made accurate determinations of the linear thermal expansion for nickel in 1941. They covered a temperature range from -196 degrees to 490 degrees Centigrade. It was found that the relation between the true thermal coefficient of expansion and temperature conformed well with the Gruneisen-Debye theory. The magnetic Curie temperature was found to be 352 degrees Centigrade. There is general agreement between their coefficient of expansion

versus temperature curve and the one plotted by Owen and Yates.

There has been some disagreement as to the crystal structure of nickel around the Curie point. However, it is generally agreed that no crystallographic transformation occurs at and is associated with the magnetic transformation.

In the last few years, the coefficient of thermal expansion of nickel has been determined quite accurately and corresponds fairly well with the calculated theoretical values at low temperatures. For higher temperatures around the Curie point, the actual values of the coefficient do not agree with the theoretical values.

The powder method of analysis was first used successfully about 1916, and was devised independently by Debye and Scherrer in Germany and by Hull in the United States. Up to that time the prevalent means of crystal structure analysis by x-rays were carried out by using the Laue and Rotation Methods. The principal disadvantage of these methods is the size of the required crystal specimen. It must be of dimensions large enough to be seen by the unaided eye. However, there are substances which do not exist as large crystals. These can not be analyzed by the above methods.

The powder method generally uses as a specimen an aggregate of microscopic crystals formed into a small cylindor. In the case of metals a fine wire may be used for the sample. The sample is rotated continuously to allow as many crystals as possible to contribute to the diffraction pattern.

A schematic diagram of a powder camera is found on

Plate I. X-rays are emitted from the target C of the tube and pass through the beryllium window A. A filter G is placed in the beam to obtain monochromatic radiation. Next the beam is collimated by the slits S_1 and S_2. The collimated beam P strikes the sample at O, where a part of it is absorbed by the sample. The remainder passes out of the camera through the exit port. The absorbed portion is re-radiated from or scattered by the sample, the coherent scattering giving rise to the diffraction lines on the film F, and the incoherent scattering producing the background on the film. The diffracted rays D, due to the coherent scattering, leave the specimen along the generators of cones concentric with the primary beam P, each cone having a semiapex angle equal to 2θ. These cones intersect the film producing arcs in pairs which are located symmetrically with respect to the primary beam. The diffraction lines have a sharp curvature for small and large values of 2θ and approach a straight line as 2θ approaches 90 degrees. Those lines for which 2θ is greater than 90 degrees are generally called back-reflection lines.

The angle 2ϕ can be determined from the incoming beam measured out to the diffraction line, and dividing it by the radius of the camera R. Since θ is the complement of ϕ, the following equation can be used to obtain θ in degrees from the arc length S:

$$\theta^\circ = 90^\circ - \frac{90S}{\pi R} \qquad (1)$$

EXPLANATION OF PLATE I

A Beryllium window

B Metal shield around target

C Target of x-ray tube

S_1 Front collimating slit

S_2 Rear collimating slit

R Radius of the camera

P Primary x-ray beam

D Diffracted x-ray beam

S Distance from primary beam to diffraction line

O Sample

G Filter

2θ Diffraction angle

2ϕ Supplementary angle of 2θ

F Film

PLATE I

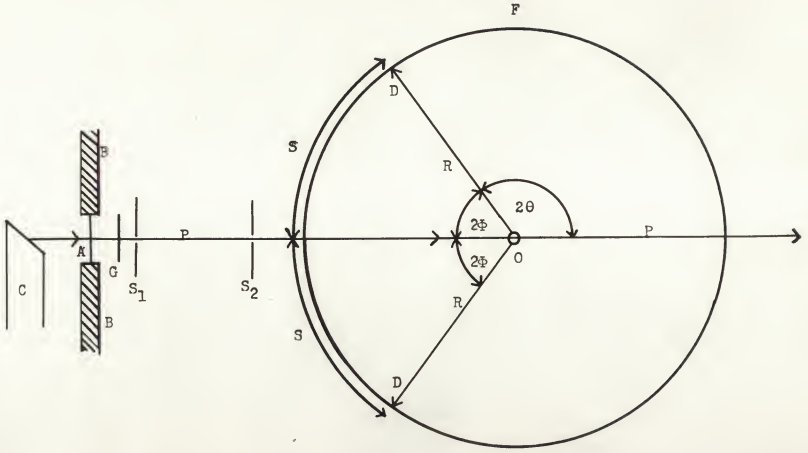

From Bragg's law:

$$n\lambda = 2d \sin\theta \qquad (2)$$

the "d" spacing is obtained for the parallel reflecting planes of atoms in the crystal associated with a particular diffraction line. The order of the diffracted line is "n" (which is generally one); λ is the wave length of the radiation producing the diffraction line; θ is one-half the diffraction angle or the glancing angle which the x-rays make with the reflecting planes; and "d" is the perpendicular distance between the parallel reflecting planes.

In a face-centered cubic crystal, under which nickel is generally classified, the lattice parameter "a" may be related to the "d" spacing by the Miller indices hkl, associated with the particular set of parallel planes which are producing the reflection. This relationship is expressed by the following equation:

$$a = d\sqrt{h^2+k^2+l^2} \qquad (3)$$

Using the above equations, one is able to calculate the lattice parameter from the known arc length S. For a given wave length the number of lines appearing on the film will be determined by the values of the "d" spacing for which $\sin\theta$, as calculated from Bragg's law, will not be greater than unity. Any set of reflecting planes whose "d" spacing gives rise to a value of $\sin\theta$ greater than one will not produce a diffraction line. For this reason a wave length is chosen to give a maximum number of diffraction lines, particularly those in the region of back reflection. These back

reflection lines are preferable for an accurate determination of the lattice parameter.

APPARATUS AND EQUIPMENT

Plate II shows the general arrangement of the apparatus as set up for operation. The control panel for the x-ray tube can be seen on the left-hand side of the picture. The potentiometer, which is used for measuring the emf of the thermocouple, is in the middle foreground. The high temperature camera is located to the left of the x-ray tube, which is found on the extreme right-hand side of the photograph. The tall black box behind the potentiometer contains the cold junction of the thermocouple. The small horizontal panel directly behind the potentiometer contains the variac controls for the furnace current. The vacuum pump, not shown in the photograph, is located on the floor under the control panel of the x-ray tube.

The X-ray Tube

The x-ray tube used for this work was a Machlett Type A-2 containing a cobalt target surrounded by a vacuum cast copper anode. Beryllium windows in the casing around the anode allowed the x-rays to be emitted on both sides of the tube at an angle of 6 degrees with respect to the plane of the target. An iron filter was used to obtain the $K\alpha$ lines and to eliminate to some extent the other radiations. Normally the tube was operated at 32 kilovolts peak voltage and at 10 milliamperes

EXPLANATION OF PLATE II

Photograph of the apparatus

PLATE II

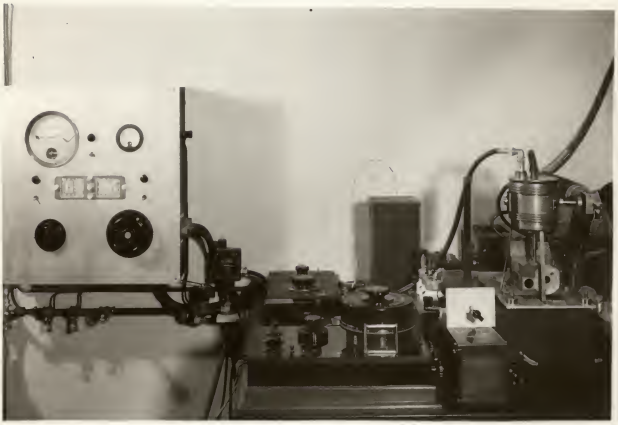

tube current. Standard methods were used to obtain and to measure the high voltage across and the current through the x-ray tube.

There were definite reasons for the selection of the cobalt tube from the following available targets: copper, cobalt, molybdenum, and tungsten. The characteristic lines of tungsten and also of molybdenum are of quite short wave length as compared to those of copper and cobalt. For short wave lengths, $\lambda < 1.0$ KX unit, the lines in back reflection would be very weak due to the rapid decrease in the atomic scattering factor with increasing scattering angle. This would, then, eliminate the Mo and W radiations. In the selection of the appropriate tube, one must consider the types of scattering encountered from the sample for a particular wave length. The two foremost types to be considered are fluorescent and coherent scattering. A wave length should be chosen such that the fluorescent scattering, which is characteristic of the sample and random in direction, does not hide the coherent scattering which gives rise to the lines of the diffraction pattern. The K_α and K_β lines of cobalt have wave lengths longer than the wave length of the K absorption edge of nickel. Thus, if cobalt radiation is used, the fluorescent scattering will be small, and the coherent scattering will be dominant. In the case of copper, the K_α line has a longer wave length than the K edge of nickel, so it could be used without difficulty. However, the K_β line of copper has a wave length slightly shorter than that of the nickel K edge. If this radiation

were used, the fluorescence would dominate over the coherent scattering. The copper K_β wave length would have some advantage for this work, because it would produce another diffraction line close to the entrance port in back reflection. However, it was ruled out due to the excessive fluorescent scattering associated with it. From Bragg's law it is seen that sin θ is directly proportional to the wave length; consequently the greatest accuracy is obtained in determining the "d" spacing from the lines having the largest diffraction angle. This is seen by differentiating Bragg's law allowing only "d" and "θ" to vary, to obtain the following:

$$\frac{\Delta d}{d} = -\cot \theta \, \Delta\theta \qquad (4)$$

where Δd is the error in the "d" spacing due to an error $\Delta\theta$ in the measurement of θ. So, as θ approaches 90 degrees, the cot θ approaches zero. Since cobalt K_α radiation and copper K_α radiation both give seven diffraction lines for nickel, the cobalt tube was selected to give the larger θ and, therefore, more precise values of the "d" spacing.

Construction of the High Temperature Camera

Two close-up pictures of the high temperature camera are shown on Plate III. Figure 1 shows a front view of the camera as it was used during operation. The furnace and the top plate are found slightly behind and to the left of the camera. The film clamps are located directly to the left of the camera. The aluminum windows are between the copper water cooling coils

EXPLANATION OF PLATE III

Fig. 1. A close-up view of the camera from the front

Fig. 2. A close-up view of the camera from above looking down

PLATE III

Fig. 1

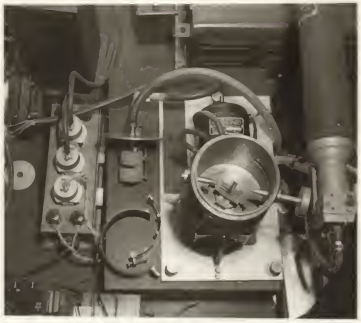

Fig. 2

on the camera. The gear box is connected directly to the drive shaft under the camera, and the motor is located behind the gear box. The entrance and exit ports can be seen protruding on either side of the camera. The x-ray tube is located to the right of the camera. Figure 2 is a top view of the camera and shows the inside of the camera. The entrance and exit ports can again be seen protruding out of and also into the camera. The centering device is found in the middle of the camera. The x-ray tube is again on the right of the camera.

The main body of the camera was made from a brass tube having an inside diameter of four and one-half inches, an outside diameter of four and three-fourths inches, and a length of four and one-half inches. Two holes three-fourths inch in diameter were drilled on opposite sides of the brass tube, their centers being exactly 180 degrees apart. Two iron mounts were soldered into the holes, forming the supports for the entrance and the exit ports. They were threaded so that a brass collar could be screwed against the ports to hold them tightly in place. The mounts were notched, and the ports were correspondingly ridged in order to obtain a good seal. A slit one-half inch wide was cut in the brass tube from the exit port mount around one side of the camera to the entrance port mount, and one-third of the distance around the opposite side from the entrance port mount back to the exit port mount. Covering this slit with one mil thick aluminum produced the necessary vacuum seal. Since the total x-ray absorption of this foil was small, the film to be exposed was clamped over the aluminum covered

slit. The slit was cut as described above so that the back reflection diffraction lines could be obtained symmetrically on both sides of the entrance port. Cooling coils consisting of quarter-inch copper tubing were wound around and soldered to the camera, three coils above the slit, and three coils below the slit.

The bottom plate of the camera was made from a circular piece of brass sheet one-eighth inch thick with a diameter equal to the outside diameter of the brass tube. The two pieces were then soldered together to form a permanent joint. A hole was cut in the center of the bottom plate, and into it a Wilson Seal (16) was soldered. The Wilson Seal permitted the use of a drive shaft through the bottom of the camera for the rotation of the sample while maintaining a vacuum seal around the shaft.

The entrance and exit ports were made from a one-half inch brass rod and turned down to a diameter of three-eighths inch leaving a ridge midway along their lengths in order to obtain a better vacuum seal. A one-fourth inch hole was drilled through the exit port along its axis, to provide an opening for the unabsorbed beam to pass from the camera without fogging the film. The exit port was later cut off outside the camera to permit alignment of the x-ray beam when the camera was completely assembled. The entrance port had a one-fourth inch hole drilled along its axis through approximately three-fourths of its length. A one-sixteenth inch hole was drilled through the remainder of the port. The entrance port was

filled with lead having a small pinhole through the lead along the axis of the port. The purpose of the pinhole was to collimate the x-rays. It was impossible to drill the pinhole through the lead, so the following method was used: A piano wire of the appropriate diameter was chosen and stretched taut by weights. The port was clamped in a vise and adjusted so that the piano wire coincided with the longitudinal axis of the port. Molten lead was then poured into the port and allowed to cool. When the lead had solidified, the wire was pulled out of the port leaving the desired pinhole along its axis.

The centering device consisted of two parts, identical in their principle of operation and construction. A groove whose cross-sectional area was trapezoidal was cut along the longitudinal axis of a rectangular block of brass, one and one-half inches long, three-sixteenths inch thick, and three-fourths inch wide. A small runner was cut from an iron bar to the same shape as the groove in the brass block. The runner was one-half inch long and formed a snug moveable fit when placed in the groove. Two end plates were fastened to the brass block, one end containing a thumbscrew. A spring between the runner and the other end plate forced the runner against the thumbscrew so it would be moved back and forth merely by turning the thumbscrew in the proper direction. One of these parts was mounted to the top of the runner of the other part and at right angles to it. This arrangement made possible transverse and longitudinal feeds with which to center the

sample. The lower brass block was fastened to the three-eighths inch drive shaft through the bottom of the camera. It was found from experience that the spring in the upper brass block did not retain its restoring properties at high temperatures, and therefore it had to be replaced by a thumbscrew in the other end plate. By operating both thumbscrews simultaneously, one was able to move the runner back and forth along the groove, still holding it tightly in position regardless of the temperature. The sample holder consisted of a one-eighth inch steel rod mounted in the iron runner of the top brass block. The wire sample was placed in a small hole drilled into the end of the rod. The sample holder extended up into the furnace a sufficient length to place only the sample in the path of the x-ray beam.

A motor and gear assembly were used to turn the drive shaft which rotated the centering device and the sample. The motor was bolted to a brass mounting plate which was fastened to the baseplate. The motor turned at a speed of forty-five rpm and was coupled into the gear box which was also bolted to the brass mounting plate. The gear box had a ratio of approximately one hundred to one; therefore, the sample was rotated at a speed of about one revolution every two minutes.

The base plate was made from sheet aluminum one-fourth inch thick. It was rectangular in shape, having a length of fifteen inches and a width of nine inches. Three leveling screws, two in adjacent corners and the third in the middle of the opposite side, were mounted in brass disks bolted to the

base plate. These enabled one to adjust the orientation of the camera to allow the x-ray beam to pass through the entrance port. Three brass legs, fastened to the base plate, supported a circular brass mounting plate. A hole was cut in the center of the mounting plate to provide an opening for the Wilson Seal which protrudes below the bottom of the camera. This allows the camera to rest on the mounting plate. Three small brass blocks containing clamp screws were soldered to the under side of the mounting plate. These screws clamped against the Wilson Seal to hold the camera tightly in place. When the screws were loosened, the camera could be rotated to obtain all possible orientations of the entrance port with respect to the x-ray tube.

The top plate was made from the same brass stock as that used for the bottom plate. The top plate had a diameter of five inches which produced an extension over the main body of the camera. It was step cut, along with the edge of the main part of the camera, to ensure a tight fit and aid in making the joint vacuum-tight. A nozzle was soldered in the center of the lid for the attachment of the hose from the vacuum pump.

The furnace was constructed from a cylinder of monel metal one and one-half inches in diameter and two and one-fourth inches in length. The inside of the cylinder was turned down to a diameter of one inch leaving a quarter inch rim on each end. A quarter inch slot was cut along the center circumference of the cylinder two-thirds of the way around to

correspond to the window slits in the main part of the camera. A three-eighths inch hole was drilled along the axis of the cylinder to provide a space inside the furnace for the sample and its holder. The furnace was wound with three layers of wire, the innermost layer constituting one heating element and the outer two layers constituting another independently controlled heating element. The inside layer contained six turns wound with No. 24 nichrome wire. Two layers of mica insulated the wire from the monel metal and from the coil wound on top of it. This element enabled one to obtain a fine adjustment of the furnace temperature by adjusting the current through it. The middle and outside layers were wound with No. 28 nichrome wire containing eight turns per layer. The wire for the middle layer was first strung with ceramic beads and then wound around the furnace. A layer of mica was placed over this winding, and the outer layer of wire was wound on top of it. A last layer of mica was then placed over this outer wire to insulate it from the iron cement, which was applied around the furnace to lower the heat losses. The ceramic beads were found necessary to increase the insulation and spacing between the layers of wire. This construction prevented short circuits between the windings as a result of the breakdown of the mica at high temperatures. This heating element provided the coarse adjustment of the furnace temperature.

The furnace was hung from a thin transite ring by three small steel rods; the transite ring, in turn, was supported by the top plate using three more small steel rods, all six rods

being displaced from their neighbors by 60 degrees. This was done to minimize the conduction of heat from the furnace to the top plate. The ends of the nichrome heating wires were fastened to heavy copper wires which were in turn soldered to the lugs of an amphenol plug. This plug was bolted to the top plate and contained four pins. Two of these pins were used for the input of the current to the two heating elements. A common ground lead returned the heater current to the current source. A small hole was drilled from the top of the furnace to a depth, half the length of the furnace. A junction of a chromel-alumel thermocouple was placed in this hole. It was assumed that it would indicate the sample temperature because of the closeness of this junction to the sample. The two leads from this junction were soldered to the remaining two pins on the amphenol plug.

Several accessories were constructed to facilitate the handling of the film used for this camera. A center punch was made to cut a hole in the film allowing it to be slipped over the brass collar which held the entrance port in place. Two envelopes were made from black paper to prevent white light from reaching the film during exposure to the x-rays. Two covers were also made from black paper to slip over the open portions of the envelopes. These covers prevented fogging of the film while it was being carried from the camera to the dark-room. A red light near the camera was used to permit the film to be changed on the camera in a darkened room. A metal clamp was constructed from brass to hold the film and envelope tightly

in place during exposure.

Operation of the High Temperature Camera

A vacuum was required inside the camera to prevent the oxidation of the sample when it was subjected to high temperatures. Nickel oxide would give rise to undesirable lines on the diffraction pattern. Reduction of heat transfer from the furnace because of the vacuum was also helpful and reduced the amount of external cooling required to prevent heat damage to the photographic film. A Cenco-Hyvac pump was used to maintain a pressure of approximately 10^{-3} millimeters of Hg inside the camera. By the use of rubber washers and vacuum wax, the entrance port, the exit port, and the amphenol plug were rendered air tight. Aluminum foil glued over the ends of the exit and entrance ports provided a seal for the holes drilled through them. Apiezon Q (black vacuum putty) was put around the joint between the top plate and the main body of the camera to eliminate any air leaks due to the joint. The aluminum windows, mentioned previously, covered the one-half inch slits around the middle of the camera, and prevented air from entering the camera through these slits. Difficulties were encountered with the aluminum windows in obtaining a piece of foil with no imperfections and in gluing the foil to the camera. These difficulties were eliminated by checking the foil beforehand for any tiny holes or tears, and by allowing the glue to dry for a period of sixty hours before applying the vacuum to the camera.

The voltage source for the furnace windings was a General Electric voltage regulator having an output rating of 750 volt-amperes. This regulator was used to eliminate fluctuations in the line voltage, thereby keeping the current through the furnace essentially constant. The ability to maintain a given temperature depended upon the regulation obtained by the voltage regulator. It was found that the voltage regulator produced good regulation most of the time, but at other times varied a small amount, producing fluctuations in the furnace temperature. The output from the regulator was applied across a five ampere variac which controlled the current through the outer heating element. An ammeter which was wired in series with this element registered the current through the element. The output was also applied across a one ampere variac which controlled the voltage across the primary winding of a 24 volt transformer. The voltage from the secondary winding was applied to the inner heating element. Thus, by adjusting the one ampere variac, the current through the inner element was varied accordingly. This current was determined by another ammeter hooked in series with this latter element.

The centering of the nickel sample was carried out using a white card placed in front of the exit port. A strong white light was incident upon the card. When looking through the pin hole in the entrance port, one was able to see the sample moving around as it was rotated by the motor. The thumbscrews on the centering device were adjusted until the wire sample remained in the center of the pinhole for a complete revolution. This

having been accomplished, the camera was rotated on the mounting plate until the entrance port was in front of the beryllium window of the tube. The camera was moved with respect to the tube and the leveling screws were adjusted until the entrance port was aligned with the x-ray beam. These adjustments allowed a collimated beam of x-rays to enter the camera. Since the pinhole of the entrance port was not exactly centered, the port was rotated in its iron mount until the collimated beam struck the sample. The centering device was also adjusted concurrently with the rotation of the entrance port until the sample remained in the center of the x-ray beam for one revolution. These final adjustments were carried out in a darkened room using a fluorescent screen to detect the beam and the shadow cast by the sample.

The remaining adjustment consisted of matching the slit in the furnace with the corresponding slits in the camera. A small arrow was scratched on the top plate during construction so that a rough setting was obtained when the arrow was pointing to the middle of the top water cooling connection. A fine adjustment was made by rotating the top plate through a small angular displacement counter-clockwise until the beam through the exit port was cut off. The top plate was then rotated slowly in a clockwise direction until the full beam appeared again at the exit port. At this position the slits were matched properly. Having matched the slits, no portion of the furnace prevented the diffracted rays from reaching the film.

The Nickel Sample

The nickel sample was in the form of a fine wire having a diameter of 0.010 inch. The wire was furnished by the International Nickel Company and was 99.9974 percent nickel. The impurities and their percentages are as follows:

Cu - 0.0002 percent

Fe - 0.0011 percent

Co - 0.0004 percent

Pb - 0.0009 percent

The surface of the wire was polished with sandpaper to eliminate any nickel oxide and any preferred orientation introduced in the extrusion of the wire. The sample was heat treated at a temperature of 400 degrees Centigrade for a short time before any diffraction pictures were taken. This was done to eliminate any strain or distortion in the wire which might have resulted when it was drawn through the die or when it was polished. It was found that this heat treatment resulted in sharper diffraction lines at all temperatures.

Temperature Measurements

The temperature of the sample was determined by means of a chromel-alumel thermocouple. The hot junction of the thermocouple was located inside the furnace in a manner previously described. A cold junction was formed by putting a chromel wire and an alumel wire into a test tube of mercury. The mercury and test tube were placed in a Dewar flash containing a mixture of

distilled water and ice made from distilled water. This established a cold reference junction at 0 degree Centigrade. The emf of the thermocouple was measured by a Leeds and Northrup Type K-2 potentiometer. A calibration table giving the emf versus temperature for a chromel-alumel thermocouple was obtained from Weber (14, Table 6, 162). This table was checked using known reference temperature points and found accurate to four significant figures.

The furnace thermocouple had to be calibrated against the true sample temperature before it could be used to measure the sample temperature. This calibration was carried out using a second chromel-alumel thermocouple, which was inserted through the exit port and fastened to the sample holder. A vacuum seal was constructed around the two thermocouple wires. The furnace was heated to a particular temperature, after which three hours were allowed for the thermocouples and the various components inside the furnace to reach equilibrium. Then, the emf of each thermocouple was measured. Knowing the emf of the sample thermocouple, the sample temperature was determined directly from the calibration chart for the thermocouples. This temperature was plotted on a graph versus the emf of the furnace thermocouple. The resulting curve is shown in Fig. 3.

Since the temperature varied due to the poor regulation of the line voltage, readings of the furnace thermocouple emf were taken often throughout an exposure. The following equation was used to calculate the mean emf of the thermocouple for the exposure:

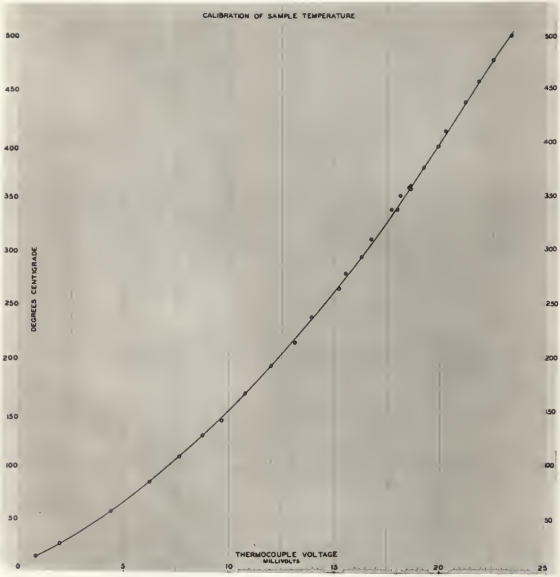

Fig. 3. Calibration curve of sample temperature versus furnace thermocouple.

$$\bar{E} = \frac{\Sigma E \Delta t}{\Sigma \Delta t} \qquad (5)$$

Where $\bar{E}$ is the mean calculated thermocouple emf, Δt is the increment of time between two thermocouple readings, and E is the average of the two readings for the corresponding Δt. The temperature of the sample was then read off the curve in Fig. 3 for the corresponding $\bar{E}$. This method gave the mean temperature of the sample for each exposure.

Preparation of the Film

A strip of film one and three-fourths inches wide and ten inches long was used for each exposure. The film was duplitized, no-screen, x-ray film manufactured by the Eastman Kodak Company. A hole was punched in each strip as mentioned previously. The average length of time to obtain an exposure was forty-eight hours. The film was developed for five minutes in the developer and fixed in the hypo for fifteen minutes. It was washed for approximately thirty minutes and then dried.

Measurement of the Film

The positions of the lines on the film were measured by a comparator on which readings could be made to an accuracy of two hundredths of a millimeter. The position on the film corresponding to the center of the entrance port was determined by measuring a pair of diffraction lines located symmetrically with respect to the primary beam and finding their center. Knowing this center position on the film, the values of the arc lengths S for all the lines were calculated from their

respective position-readings.

EXPERIMENTAL RESULTS

Radius Calibration of the Camera

Before any diffraction pictures could be analyzed, it was necessary to determine accurately the radius of the camera. To do this, several diffraction pictures were taken of nickel at room temperature, and the arc lengths S on the films were measured five times for each line. For a particular line, all the S values from these films were averaged to obtain a mean arc length for that line. This was done for every diffraction line on the film. Assuming that "a" is equal to 3.5169 KX units (1, App. VII, 553) for room temperature (16 degrees Centigrade), the exact values of 2ϕ in radians for each line were obtained by computing backwards through the powder method of analysis as outlined earlier in this paper. The value of the radius for each line was then obtained by dividing the average S for the line by the respective value of 2ϕ. At higher temperatures the lines shifted toward the exit port, but it was assumed that the value of R for each particular line remained constant in spite of the small shift of the line to a new position on the film. The values of R for each line along with their associated hkl values and wave lengths are listed in Table 1. The wave length for lines 4 and 6 is that of the $K_{\alpha 1}$ line of cobalt. The wave length for lines 5 and 7 is that of the $K_{\alpha 2}$ line. The wave length for lines 1, 2, and 3 is a

weighted mean of the $K\alpha_1$ and $K\alpha_2$ wave lengths of cobalt. This weighted mean was calculated by the following equation:

$$\lambda_{av} = \frac{2\lambda_{\alpha 1} + \lambda_{\alpha 2}}{3} \qquad (6)$$

The values in Table 1 were used for the calculation of the lattice parameter for each line. The lines and their respective numbers are shown in Plate IV, Figs. 6 and 7. These are prints from two films exposed at different sample temperatures. The shift in the back reflection lines (Nos. 4, 5, 6, and 7) can be detected.

Table 1. Values of the radius, wave length, and hkl values for each diffraction line.

Line no.	R(mm)	λ(KX)	hkl
1	60.165	1.7866	111
2	60.110	1.7866	200
3	60.104	1.7866	220
4	60.112	1.7853	311
5	60.031	1.7892	311
6	60.129	1.7853	222
7	59.987	1.7892	222

Measurements of the Lattice Parameter

After the radius was calibrated, diffraction pictures were taken at various sample temperatures, and the lattice parameter computed for these temperatures. Table 2 lists the values of the lattice parameter for their respective temperatures. These

values of the lattice parameter were plotted versus temperature. A smooth curve was drawn through the points and is shown in Fig. 4. The value of the lattice parameter at 0 degree Centigrade was obtained from this graph by extrapolating the curve through 0 degree Centigrade. The intersection of the curve with the vertical axis determined "a_o" directly.

Linear Coefficient of Thermal Expansion

The linear coefficient of expansion is related to the slope of the curve plotted in Fig. 4. The relationship between the lattice parameter and the temperature is:

$$a = a_o (1 + \alpha t) \qquad (7)$$

where "a" is the lattice parameter at a temperature "t", "a_o" is defined above, and α is the linear coefficient of thermal expansion referred to 0 degree Centigrade. Differentiating equation (7) with respect to temperature, one obtains:

$$\alpha = \frac{1}{a_o}\left(\frac{da}{dt}\right) \qquad (8)$$

which is a relationship between the desired coefficient and the slope $\left(\frac{da}{dt}\right)$ of the curve in Fig. 4. The slope was obtained directly from the curve for various temperatures, and from them the values of α were calculated. These values were plotted versus their respective temperatures, and a smooth curve was drawn among the points. This resulted in the upper curve in Fig. 5, which shows the variation of the linear coefficient of thermal expansion with respect to temperature. The lower curve in Fig. 5 represents a portion of the Grueneisen-Debye theoretical curve as calculated for nickel by Nix and MacNair (11).

Table 2. Values of the lattice parameter and their respective temperatures.

Temperature Degrees centigrade	Lattice parameter KX units
0	3.5163
16	3.5169
79.5	3.5208
176	3.5248
235	3.5307
299.5	3.5336
316	3.5347
323	3.5355
336	3.5358
345	3.5374
346	3.5370
352	3.5378
362	3.5383
371	3.5392
377	3.5398
400	3.5408
428	3.5419

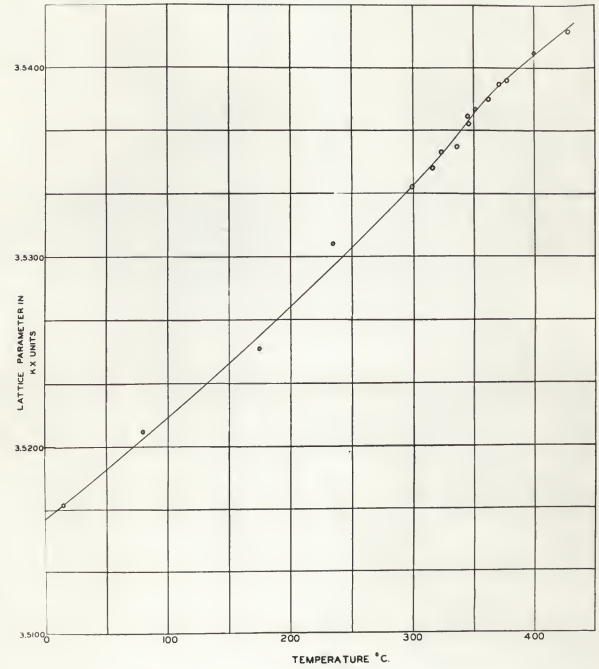

Fig. 4. Plot of the lattice parameter of nickel versus temperature.

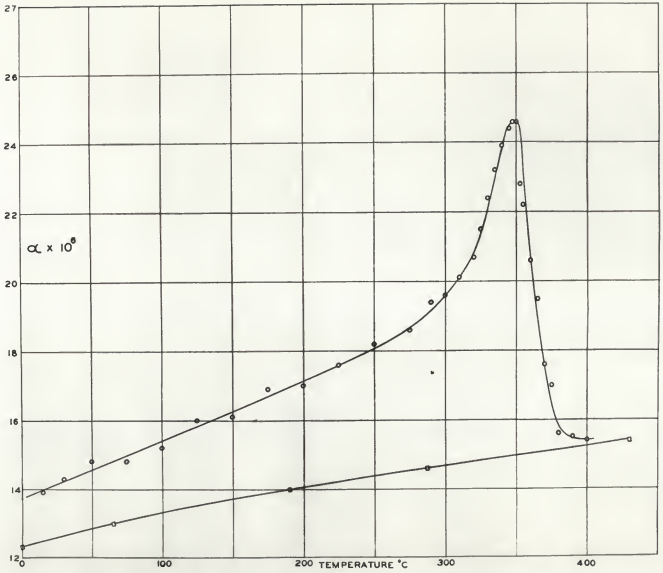

Fig. 5. Graph of the linear coefficient of thermal expansion versus temperature.

EXPLANATION OF PLATE IV

Fig. 6. Print from exposed film showing diffraction lines and their respective numbers for a sample at a temperature of 362 degrees Centigrade.

Fig. 7. Print from exposed film showing diffraction lines and their respective numbers for a sample at a temperature of 16 degrees Centigrade.

PLATE IV

Fig. 6.

Fig. 7.

Experimental Errors

There were four main sources of error present throughout this research project. There are (I) errors in the measurement of the film, (II) systematic errors of the powder camera, (III) errors in the temperature measurements, and (IV) errors resulting from drawing the experimental curves.

In the case of the film measurements, it was found that the greatest source of error was in setting the hairline of the comparator lens over the center of a diffraction line. This became quite pronounced in the case of lines of weak intensity. The error in reading the comparator was small compared to the former, provided one looked through the lens properly to eliminate parallax. The lines on a film were measured three times, and these values averaged to obtain the arc length S for each line. This reduced the error in the measurements of S considerably, making it insignificant with respect to the other types of error.

The systematic errors of a powder camera can be listed as follows: (1) film shrinkage, (2) errors in measuring the camera radius, (3) displacement of the specimen from the center of the camera by improper adjustment, (4) displacement of the effective center of the specimen from the center of the camera by absorption of the rays in the sample, (5) x-ray beam divergence, and (6) deviations from Bragg's law due to the refraction of x-rays. The first two are the predominant types of error under this classification. It was assumed that the method of the radius

calibration would compensate for these errors by absorbing them into the value of the effective radius for each line. Also the values of the lattice parameter were computed primarily from the lines in back reflection, for which these systematic errors become small. It was shown earlier that these errors are proportional to cot θ and approach zero as θ approaches 90 degrees. However, the systematic errors were not completely eliminated. These errors could have been reduced even further by selecting a longer wave length and thus shifting the lines farther into back reflection. This would allow the use of extrapolation methods (1, 135) to eliminate the systematic errors.

The errors in the temperature measurements contributed considerably to the total error of the problem. These errors were due to several causes. If the conditions of the camera (such as the vacuum inside the camera and the temperature of the main body of the camera) during calibration were different from the general operating conditions, the thermal gradients inside the camera during operation would be different from those existing during calibration. This would possibly give rise to slightly different sample temperatures from those for which the furnace thermocouple was calibrated. This error could be reduced by recalibrating the furnace thermocouple periodically, eventually obtaining an average curve which would be good for the normal operating conditions of the camera. The current fluctuated through the heating elements as mentioned previously. These fluctuations probably did not cause too much effect on the sample temperature due to the thermal capacity of the furnace. The

primary source of error resulted from a prolonged decrease or increase of the current from its initial value as set at the beginning of each exposure. This error was reduced by calculating the mean emf of the thermocouple as described earlier. Error was also introduced in obtaining the temperature from the calibration curve in Fig. 3 since it is an experimental curve.

The drawing of the experimental curves also contributed some error to the final results. Smooth curves were drawn for each set of data, even though all the experimental points did not lie on these drawn curves. In the case of the lattice parameter versus temperature curve (Fig. 4), there were not enough points ascertained in the region from 0 degree Centigrade to 250 degrees Centigrade to specify the curve in more detail and more accurately over this range. Also small errors were introduced when the slope was determined from the lattice parameter versus temperature curve. The primary source of error under this heading can be attributed to the drawing of the lattice parameter curve, since the values of α depend directly upon the slope of this curve.

CONCLUSIONS

The coefficient of thermal expansion versus temperature curve shows a maximum value for α at a temperature of 349 degrees Centigrade. This temperature is the Curie temperature as determined by this experiment. The value of α at this temperature is found to be $24.4 \times 10^{-6} \text{degree}^{-1}$. The values of α in the lower temperature region are not as dependable as those for temperatures around the Curie point, since the lattice parameter curve in that region is based upon fewer experimental points. Within the limits of experimental error, these results are in general agreement with those of earlier investigations on the subject.

The structure of nickel remained face-centered cubic over the entire range of the temperatures investigated. However, additional exposures over small intervals of temperature would have to be obtained, before the conclusion could be made that no other forms of nickel are present in the region of the Curie point.

ACKNOWLEDGMENT

Acknowledgment is extended to Dr. R. D. Dragsdorf for his excellent advice and helpful criticisms regarding the construction of the camera and during the progress of this problem. Appreciation is also expressed to Professor E. V. Floyd for the construction of the Wilson Seal. The International Nickel Company generously donated the high purity nickel wire which was used for this project.

BIBLIOGRAPHY

(1) Barrett, Charles S.
Structure of metals. New York. McGraw-Hill. 1943.

(2) Bredig, G. and E. Schwarz von Bergkampf.
Hexagonal nickel. Ztschr. f. Phys. Chem., 155: 172-176. 1931.

(3) Cardwell, A. B.
Photoelectric and thermionic properties of nickel. Phys. Rev., 76: 125-127. 1949.

(4) Compton, A. H. and S. K. Allison.
X-rays in theory and experiment. New York. D. Van Nostrand. 1935.

(5) Del Nunzio, B.
Crystal lattice of nickel and the sudden change in magnetic properties. Atti. ist. Veneto, 92: 541-549. 1933.

(6) Del Regno, W.
Transformation of nickel in the neighborhood of the Curie point. Atti. accad. Lincei, 1: 179-181. 1925.

(7) Ewert, M.
Specific heats and the allotropism of nickel between 0° and 1000°. Proc. Acad. Sci. Amsterdam, 39: 833-838. 1936.

(8) Jesse, William P.
X-ray crystal measurements of nickel at high temperatures. Physics, 5: 147-149. 1934.

(9) Koester, Werner and Winifried Schmidt.
Relation between lattice parameter and ferromagnetism. Arch. Eisenhüttenw, 8: 25-27. 1934.

(10) Mazza, L. and A. G. Nasini.
The crystal structure of nickel. Phil. Mag., 7: 301-311. 1929.

(11) Nix, F. C. and D. MacNair.
Thermal expansion of pure metals: copper, gold, aluminum, nickel, and iron. Phys. Rev., 60: 597-605. 1941.

(12) Owen, E. A. and E. L. Yates.
X-ray measurement of the thermal expansion of pure nickel. Phil. Mag., 21: 449-457. 1929.

(13) Sizoo, G. J.
Crystal size and magnetic properties of pure nickel. Z. Physik, 53: 449-457. 1929.

(14) Weber, Robert L.
Temperature measurements. Ann Arbor, Michigan. Edwards Brothers. 1948.

(15) Williams, Clarke.
Thermal expansion and the ferromagnetic change in volume of nickel. Phys. Rev., 46: 1011-1014. 1934.

(16) Wilson, Robert R.
A vacuum-tight sliding seal. Rev. of Sci. Instru., 12: 91-93. 1941.